UNIVERSITÀ DI PISA

FACOLTÀ DI INGEGNERIA

RELAZIONE PER IL CONSEGUIMENTO DELLA LAUREA SPECIALISTICA IN INGEGNERIA MECCANICA

Design and development of Electro Chemical Milling System (ECMIL)

RELATORI

Prof. Ing. Michele Lanzetta
Dipartimento di Ingegneria Meccanica, Nucleare e della Produzione

Dr Anjali de Silva
School of Engineering and Computing Glasgow Caledonian University

IL CANDIDATO

Luca Del Moro

Sessione di Laurea del 11/05/2011
Anno Accademico 2009/2010
Consultazione consentita

Contents

Abstract

The following thesis contains the report of the work done in association with Glasgow Caledonian University and it is about designing and developing of a non-conventional machining system aimed on using electro chemical reactions for milling processes, called Electrochemical Milling System (ECMIL).

This represents an evolution of an existing process, never developed because of several technical problems.

The aim of the thesis is demonstrating process feasibility by experimental tests and build up bases for process improvement.

Tests had been made using a simple and cheap system comparing to the classic ECM process.

The tool had been moved in one unique direction, saving its handling on a plane for future works.

Satisfying results had been obtained, though used machining parameters are different to the calculated ones; this is mainly caused by the way the electrolyte passed through the working area, allowing a not proper current transfer.

This last aspect future works will focus on.

Keywords

ECM, Tool, Unconventional machining, Milling

1. Introduction

In the machining field non-conventional machining processes are getting used more and more; these are different from conventional machining because the tool doesn't touch the work piece during the machining.
The most popular systems can be distinguished each other by the kind of energy used for the machining:

Mechanical:	Ultrasonic Machining
	Water Jet Machining
	Abrasive Water Jet Machining
Electrochemical:	Electrochemical Machining
	Electrochemical Grinding
Electro-thermal:	Electro-discharge Machining
	Electron Beam Machining
	Laser Jet Machining
Chemical:	Chemical Milling
	Photochemical Milling

Some of these techniques are frequently used despite of their costs for setting-up and utilization thanks to the high application range and to the high precision and repeatability of the process; an example is given by laser technology, in engineering is used for cutting, welding, stereo lithography and measuring operations, but it can also find medical applications.
If laser technology is very versatile on one side, on the other side its thermal nature produces an heat affected zone (as commonly happens during welding processes) which may be detrimental to the component.
Many studies have been made on Electrochemical Machining because the process takes place anyhow material's mechanical and thermal properties are, allowing to work on extremely hard or high melting point materials getting very smooth surfaces without modifying material's properties.

The machining changes name depending on the aim of use; each one of them is characterized by a properly designed tool and tool handling system, restricting use variability, and the tool moves by only one direction.

- Shaped Tube Electrolytic Machining

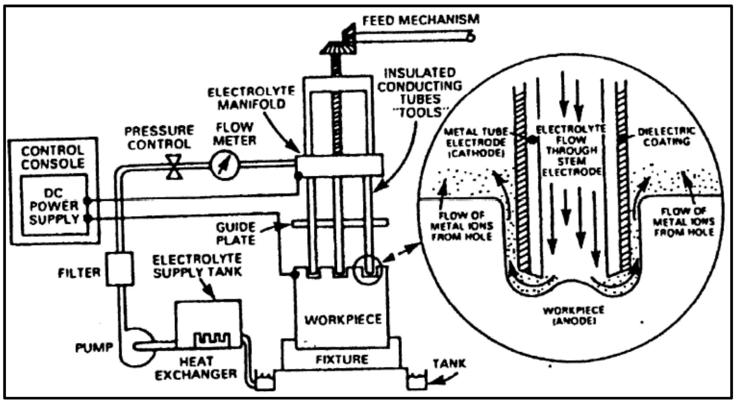

Image 1.1

- ElectroChemical Grinding

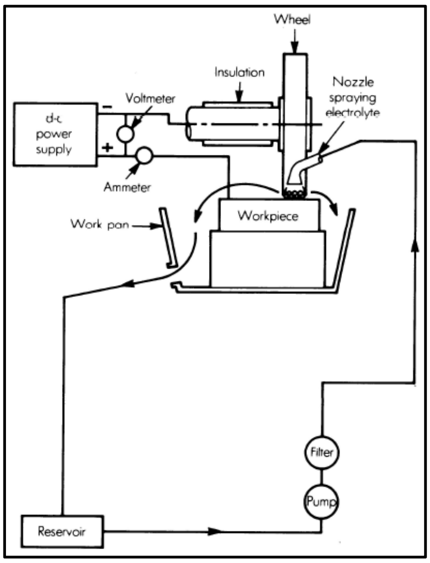

Image 1.2

- Electro Chemical Deburring

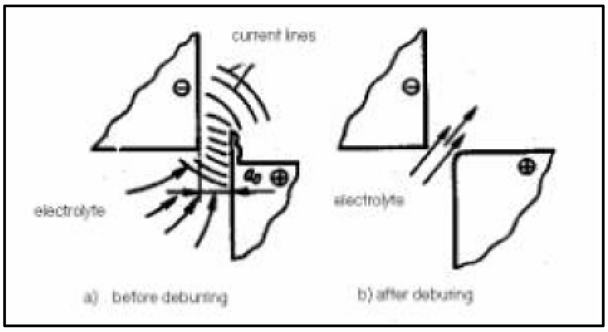

Image 1.3

- CNC Electro Chemical Machining

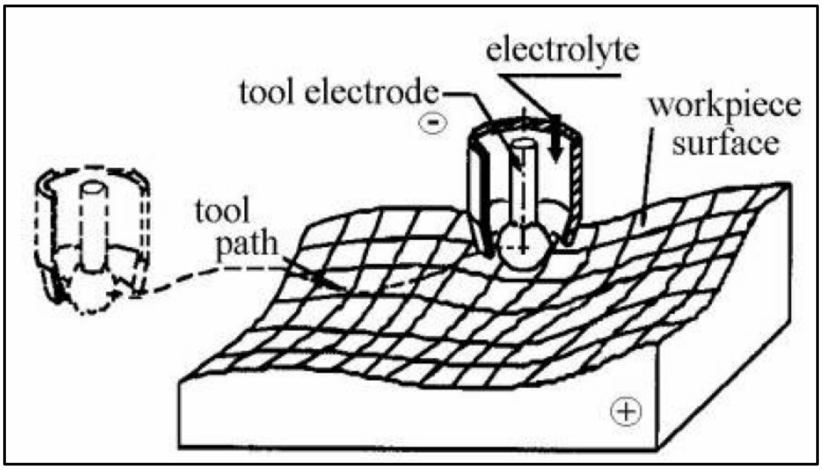

Image 1.4

- Electro Chemical Honing

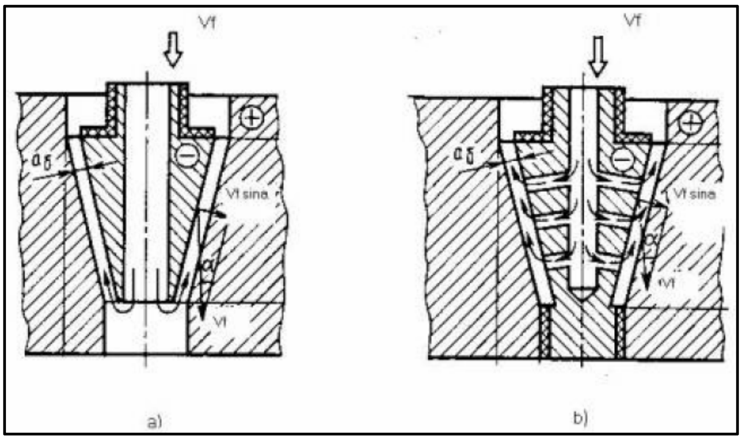

Image 1.5

From what has just been said can be deduced that if a new technique to exploit electrochemical energy with a simple, versatile and three axes moving tool would be developed, an extremely flexible machine could be achieved, able to do cutting operations, called Electro Chemical Milling.

Preliminary studies [5] [12] [19] [21] had been done on micro milling operations because the machining is hardly achieving on “macro” due to several problems which will be showed afterwards.

1.1. Principles

When a voltage is applied between two metal electrodes which are immersed in an electrolyte, current flows through the electrolyte from an electrode to the other one. Unlike the conduction of an electric current in a metal, in which only the electrons move through the structure of the material, “ions”, electrically charged groups of atoms, migrate physically through the electrolyte and in so doing carry the current. The transfer of electrons between the ions and electrodes completes an electrical circuit and also brings about the phenomenon of metal dissolution at the positive electrode, or “anode”; this is the basis of metal removal in the Electro Chemical Machining process.

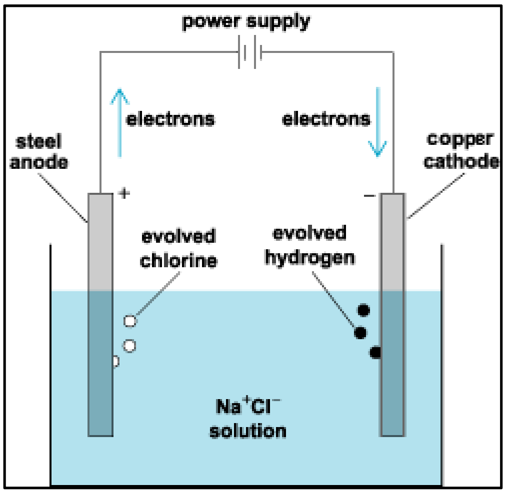

Image 1.6

Cathodic reaction

$2H^{+} + 2e^{-} \rightarrow H_2$ (gas)

Anodic reaction

$Fe - 2e^{-} \rightarrow Fe^{2+}$

Reactions in the electrolyte

$H_2O \rightarrow (OH)^{-} + H^{+}$

$NaCl \rightarrow Na^{+} + Cl^{-}$

$Fe^{2+} + 2Cl^{-} \rightarrow FeCl_2$

$FeCl_2 + 2(OH)^{-} \rightarrow 2Cl^{-} + Fe(OH)_2$ (called *anodic sludge*)

$Na^+ + (OH)^- \rightarrow Na(OH)$

Using the Faraday's law is it possible to establish the exact volume dissolved related to the current involved, time of application and material properties:

$$V = \frac{I \cdot t \cdot N}{F \cdot n \cdot \rho}$$

Where:

$V = dissolved\ volume$

$I = current$

$t = time$

$N = atomic\ weight$

$F = Faraday\ constant = 96500\ A \cdot secs$

$n = atomic\ valency$

$\rho = density$

The amount of volume dissolved in a time unit is called *dissolution rate*.

In the Faraday's law is easy to recognise that the dissolved volume depends on two variable parameters – current and time – and some constant terms once the working piece material has been chosen.

All these constants can be grouped in a unique constant called s*pecific volume*:

$$V_S = \frac{N}{F \cdot \rho \cdot n}$$

Electrolyte has its own resistivity and it is obtained by tests; it depends on salt concentration, salt type and electrolyte temperature, e.g. 12% NaCl electrolyte at 60°C has a resistivity $r = 4\ \Omega\ cm$

Electrolyte resistance depends on the gap between two electrodes and on the section area where the current passes through, as deduced from second Ohm's law:

$$R = \frac{g \cdot r}{A}$$

In this doing the current involved can be calculated knowing geometrical parameters and the voltage applied on both electrodes using first Ohm's law:

$$I = \frac{E}{R} = \frac{\eta \cdot E \cdot A}{g \cdot r}$$

The term η in the previous equation represent operation efficiency; it is used due to the *electrodes passivation* effect: it is a phenomenon involving metal surface natural covering by a metallic oxide layer which is very resistant and adhesive on the surface itself. This layer, insoluble in water and low chemical reactive, avoids hydrogen to go in touch to metal, therefore slowing down and decreasing voltage between electrodes in the electrolyte.

This effect is prevented switching polarity periodically, so anodic dissolution is exploited to remove the created oxide layer.

1.2. Feed rate

In a traditional ECM process the section area is fixed, so the volume can be assumed dissolving linearly.

From the previous equation can be deduced that a constant current is achieved only if the gap is constant, it means that the tool as to move linearly as fast as the anodic dissolution involves to obtain a steady state machining.

Combining Faraday's and Ohm's laws the steady state feed rate is equal to:

$$f = \frac{N \cdot E \cdot \eta}{F \cdot n \cdot g \cdot r \cdot \rho} = \frac{Cost}{g}$$

1.3. Electrolyte

Analyzing the chemical reactions in the electrolyte can be noticed that a solid deposit is obtained as reaction product, that could compromise the current transfer so there is the need to keep it away from the working area. This is obtained using a continuous electrolyte flow, able to flush all the impurities and feed the system with new electrolyte.

As already said the electrolyte as its own resistance, so it warms up due to Joule effect; temperature increasing is given by the equation:

$$\Delta T = \frac{R \cdot I^2}{g \cdot \omega \cdot v \cdot \rho_{el} \cdot c}$$

With:

$\omega = electrolyte\ channel\ width$

$v = electrolyte\ speed$

$\rho_{el} = electrolyte\ density$

$c = specific\ heat$

Using current density $J = \frac{I}{A}$ and the second Ohm's law, the equation turns in:

$$\Delta T = \frac{r \cdot J^2 \cdot \Delta x}{v \cdot \rho_{el} \cdot c}$$

$\Delta x = electrolyte\ channel\ length$

Electrolyte resistivity depends on the temperature:

$$r = \frac{r_0}{1 + \alpha \cdot \Delta T}$$

$r_0 = standard\ conditions\ resistivity; usually\ is\ 7\ \Omega \cdot cm$

$\alpha = thermal\ conductivity = 0.02\ °\mathrm{C}^{-1}$

The slower is the electrolyte flow the bigger will be the heating, it is necessary to prevent its boiling. Temperature increasing produces also resistivity decreasing causing current raising, so there's the need to modify working gap to keep feed rate constant or increasing feed rate to keep gap constant; in both of cases the process is not steady anymore.

There is a practical limit to the maximum temperature, which is 70°C; electrolyte heating has to be low to avoid too big resistivity value modification, so it creates bindings to the minimum speed:

$$v = \frac{r_0 \cdot J^2 \cdot \Delta x}{\Delta T(1 + \alpha \cdot \Delta T) \cdot \rho_{el} \cdot c}$$

To achieve a better flush in the working area the electrolyte has to be in turbulent flow condition, it means that Raynolds' number must be over 3000:

$$Re = \frac{\rho_{el} \cdot v \cdot D}{\mu}$$

$D = hidraulic\ diameter = 2 \cdot g\ for\ flat\ channels$

$\mu = viscosity$; $1.2 \cdot 10^{-2} \frac{g}{cm \cdot sec}$ at 20 °C; $0.6 \cdot 10^{-2} \frac{g}{cm \cdot sec}$ at 60 °C

A new condition of minimum speed is obtained, the highest one will be chosen.

The pressure needed to contrast viscous forces is given by a sperimental equation:

$$p = \frac{0{,}3164 \cdot \rho_{el} \cdot v^2 \cdot \omega}{2 \cdot D \cdot Re^{0.25}}$$

This value is important to establish pump characteristics.

An important choice about electrolyte's concentration has to be made, in fact its own *conductivity* $\chi = \frac{1}{r}$ depends strictly on the concentration, as shown in Image 1.7:

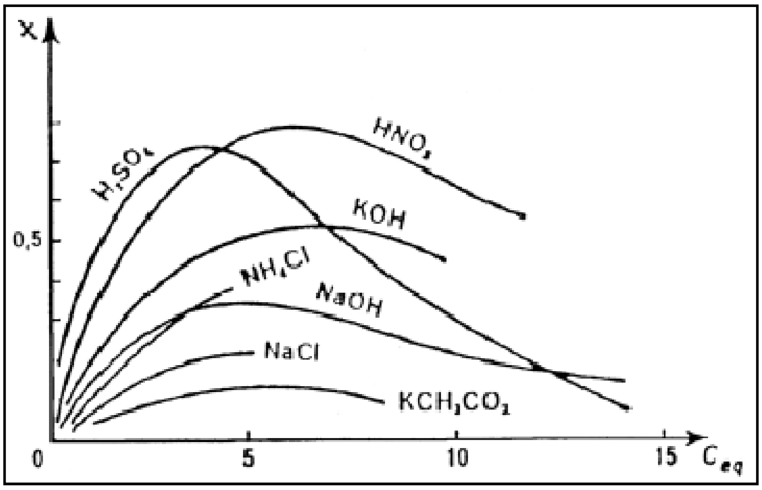

Image 1.7

1.4. Tool design

From what has been just said we can assume that material dissolution proceeds in the tool surface perpendicular direction, final shape therefore is closely connected to the tool shape.

Actually the opposite process is used, tool shape is adapted for creating the desired surface.

The tool has a fixed shape and it moves through one way at the previously calculated speed, directly connected to the current involved in the machining.

From Image 1.8 can be noticed that if a tool face is not perpendicular to feed direction the speed which it approaches the workpiece is different, so there’s a gap modification and a consequent dissolution rate modification; the process is not steady anymore:

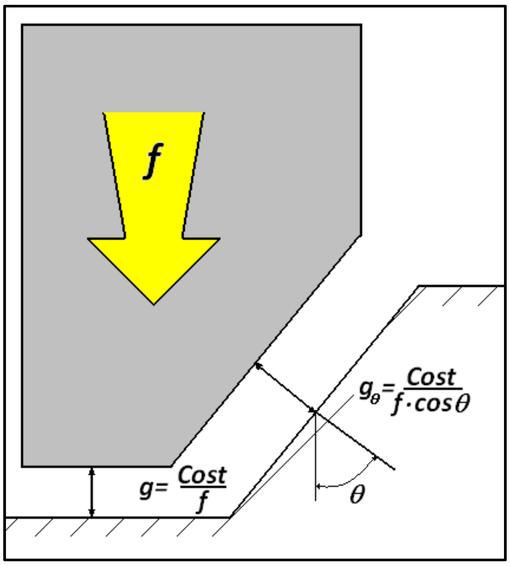

Image 1.8

Tool has to be modified as to obtain the same dissolution rate through an only direction.

A consideration more has to be pointed up: if tool surface is parallel to feed direction gap tends to go to the infinite getting parabolic shape (as shown in Image 1.9).

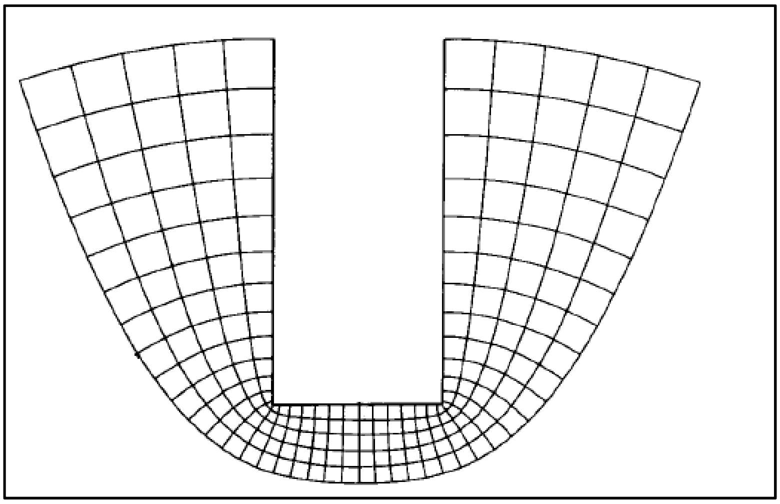

Image 1.9

Usually tool's side surfaces are electrically insulated.

The tool needs to be made with high resistance materials due to high pressure involved in the process.

2. Design

First of all a Cartesian coordinate system has to be defined.

Usually for mechanical processes ***Z*** axis is defined as parallel to the chuck axis, positive is the tool is leaving the workpiece; the remaining axes have to be taken as they define the coordinate system.

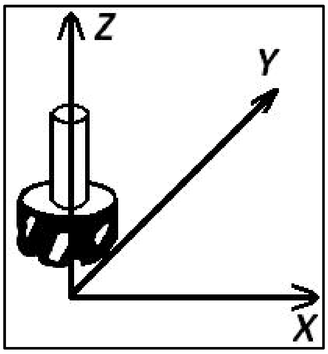

Image 2.1

The aim of this project is finding a way to improve electrochemical machining potentialities; proving that creating slots in a steel piece is possible by using a simple tool like a copper tube, which moves in every direction in ***X-Y*** plane.

Feed direction changes, so front gap and side gap swap their position compared to the tool.

Using a tube creates dimensional precision problems, in fact the part which moves perpendicularly to the feed direction is geometrically a line:

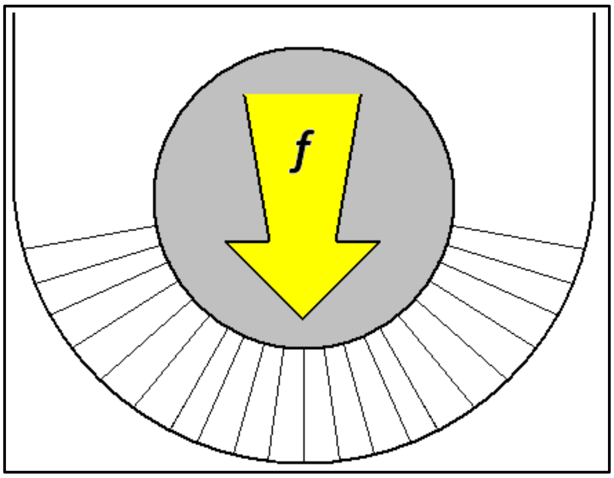

Image 2.2

The corner is still a transition area, as shown in Image 2.3**Errore. L'origine riferimento non è stata trovata.**:

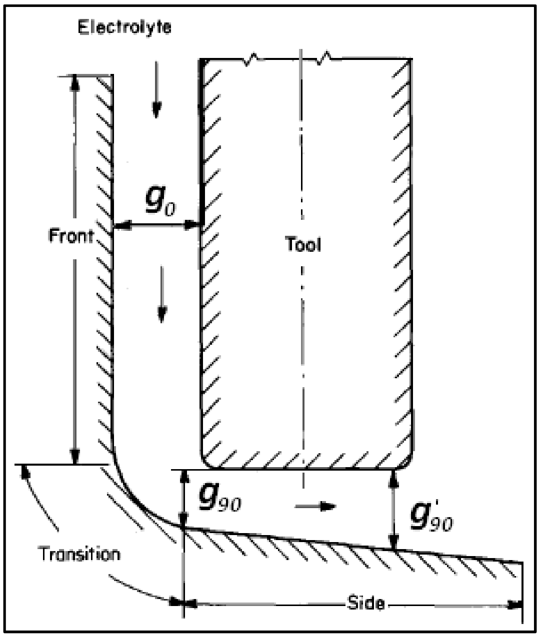

Image 2.3

Experimental results [13] provide an approximate formula of the gap evolution in all directions with the stationary tool:

$$g = g_0 + \frac{\eta \cdot J}{F \cdot \rho} \cdot t$$

$$g_{90} = 0.19536 \cdot g + 0.5779$$

$$g'_{90} = (2 \cdot z \cdot g + g_{90}^2)^{0.5}$$

In this way it is possible to establish approximately slot oversize.

Following approximations on working parameters will be taken because the main aim is proving a brand new process feasibility and as so could be effected by important changes during tests.

For an easier calculation two worksheets have been created in which the feed speed is calculated by the change in voltage with a constant gap (Chart 2.1)and by the change in starting gap with a constant voltage (Chart 2.2).

Chart 2.1

N	E	η	r	F	n	ρ	z		Costant	g_0	feed rate
g	V		$\Omega \cdot mm$	$A \cdot sec$		$\frac{g}{mm^3}$	mm		$\frac{\eta \cdot E \cdot N}{r \cdot F \cdot n \cdot \rho}$	mm	$\frac{mm}{s}$
56	12	0.8	0.5	96500	2	0.00787	5		0.707876043	0.5	1.4157520854
56	**13**	**0.8**	**0.5**	**96500**	**2**	**0.00787**	**5**		**0.766865713**	**0.5**	**1.5337314258**
56	14	0.8	0.5	96500	2	0.00787	5		0.825855383	0.5	1.6517107663
56	**15**	**0.8**	**0.5**	**96500**	**2**	**0.00787**	**5**		**0.884845053**	**0.5**	**1.7696901067**
56	16	0.8	0.5	96500	2	0.00787	5		0.943834724	0.5	1.8876694472
56	**17**	**0.8**	**0.5**	**96500**	**2**	**0.00787**	**5**		**1.002824394**	**0.5**	**2.0056487876**
56	18	0.8	0.5	96500	2	0.00787	5		1.061814064	0.5	2.1236281281
56	**19**	**0.8**	**0.5**	**96500**	**2**	**0.00787**	**5**		**1.120803734**	**0.5**	**2.2416074685**
56	20	0.8	0.5	96500	2	0.00787	5		1.179793404	0.5	2.3595868090
…	**…**	**…**	**…**	**…**	**…**	**…**	**…**		**…**	**…**	**…**

Chart 2.2

N	E	η	r	F	n	ρ	z		Costant	g_0	feed rate
g	V		$\Omega \cdot mm$	$A \cdot sec$		$\frac{g}{mm^3}$	mm		$\frac{\eta \cdot E \cdot N}{r \cdot F \cdot n \cdot \rho}$	mm	$\frac{mm}{s}$
56	16	0.8	0.5	96500	2	0.00787	5		0.943834724	0.1	9.4383472358
56	**16**	**0.8**	**0.5**	**96500**	**2**	**0.00787**	**5**		**0.943834724**	**0.11**	**8.5803156690**
56	16	0.8	0.5	96500	2	0.00787	5		0.943834724	0.12	7.8652893632
56	**16**	**0.8**	**0.5**	**96500**	**2**	**0.00787**	**5**		**0.943834724**	**0.13**	**7.2602671045**
56	16	0.8	0.5	96500	2	0.00787	5		0.943834724	0.14	6.7416765970
56	**16**	**0.8**	**0.5**	**96500**	**2**	**0.00787**	**5**		**0.943834724**	**0.15**	**6.2922314906**
56	16	0.8	0.5	96500	2	0.00787	5		0.943834724	0.16	5.8989670224
…	**…**	**…**	**…**	**…**	**…**	**…**	**…**		**…**	**…**	**…**

It has been chosen to supply electrolyte to the system from within the tool, as it is in the electrochemical drilling process; the fluid reaches the working area by a hole created on the tool side and this has led to an important choice regarding process parameters: to ensure the fluid directionality out of the working area it has been chosen to have a laminar flow ($Re < 3000$), so instead of having two minimum speed bindings it is obtained an acceptability range.

The laminar flow choice leads to a new pressure to counter the forces of inertia:

$$\Delta p = \frac{64}{Re} \cdot \frac{\rho_{el} \cdot v^2 \cdot \Delta x}{2 \cdot D}$$

2.1. Electrolyte system

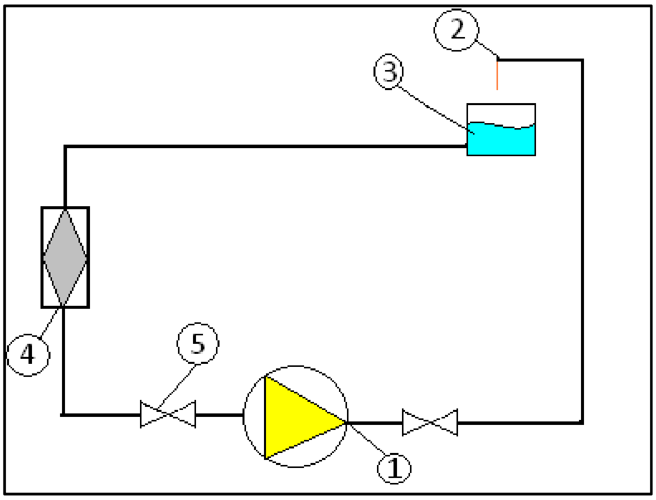

Image 2.4

1. Pump
2. Tool
3. Collecting tank
4. Filter
5. Valve (x2)

The scheme drawn in Image 2.4 showing the electrolyte circulation system is very simple; nevertheless it represents one of the main points to achieve a good quality machining.

Below is reported an example of a worksheet used to calculate limit speeds depending on starting gap:

Chart 2.3

μ_e	ρ_e	g_0	E-ΔE	C_{se}	χ_0	α	Δx		v(Re)			v(ΔT)	
Pa s	kg/m^3	m	V	J/kg°C	Ω^{-1}m^{-1}	°C^{-1}	m		m/s	km/h		m/s	km/h
0.003	1000	0.00014	12	4186	16	0.02	0.004		32.14	115.71		13.48	48.53
0.003	1000	0.0002	12	4186	16	0.02	0.004		22.50	81.00		6.60	23.78
0.003	1000	0.00025	12	4186	16	0.02	0.004		18.00	64.80		4.23	15.22
0.003	1000	0.0003	12	4186	16	0.02	0.004		15.00	54.00		2.94	10.57
0.003	1000	0.0004	12	4186	16	0.02	0.004		11.25	40.50		1.65	5.94
0.003	1000	0.0005	12	4186	16	0.02	0.004		9.00	32.40		1.06	3.80

$$\chi_0 = \ electric\ conductivity = \frac{1}{r_0}$$

Limit speed able to satisfy laminar flow condition has been obtained using $Re = 3000$.

Since this range has to be respected, electrolyte speed ingoing to the gap is chosen as arithmetic intermediate between two extremes:

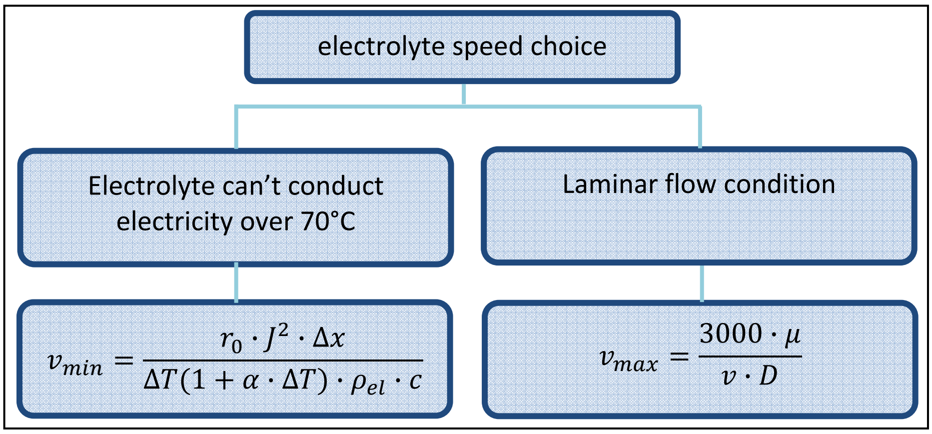

Image 2.5

Chart 2.4

Average value	Corresponding Reynolds' number:
m/sec	
22.81109529	2129.035561
14.55243669	1940.324892
11.11355948	1852.259914
8.967749642	1793.549928
6.450609173	1720.162446
5.028389871	1676.129957

Electrolyte pressure at the inlet is given by:

$$P_{el} = \frac{1}{2} \cdot \rho_{el} \cdot v^2 + \Delta p$$

Using mass conservation principle and assuming to feed the system through a 6mm diameter tube fluid speed outgoing from the pump can be calculated, from which flow rate, pressure and power to make the system work are deduced.

$$v_{pump} = \frac{v_{average} \cdot \pi \cdot g_0^2}{\pi \cdot 0.003^2}$$

$$Flow = v_{pump} \cdot \pi \cdot 0.003^2$$

$$W_{pump} = Flow \cdot (P_{el} + \Delta p_{idr})$$

Δp_{idr} represents hydraulic loss of pressure, either concentrated (valves, curves, etc..) or distributed inside pipes.

The first assumption for the experiment is using starting gap $g_0 = 0.14\ mm$, from which average speed value is deduced and is $v_{average} = 22.81\ \frac{m}{sec}$.

The pump has to provide $0.38\ MPa = 3.8\ bar$ pressure and $1.4\ \cdot 10^{-6} \frac{m^3}{sec}$ flow rate.

Values just obtained are smaller than often used ones because system's dimensions are shrunk.

The fluid outgoing from the working area must be filtered before its re-using because anodic sludge could prejudice the proper pump running. It must be used a filter able to collect $70\eta m$ of average dimension particles.

Practise suggests to use 12% concentrated $NaNO_3$ electrolyte; although 12% concentrated NaCl solution had been chosen due to unavailability during test period, it is still able to transfer current, but creates corrosion problems, as can be noticed in Image 2.7 and Image 2.9.

For the preliminary phase a circulation pump had been used, its flow rate was constant at equipped with a small internal filter and a storage tank.

2.2. Electrical system

Practice recommends the use of current density $J\ from\ 1\ to\ 10 \frac{A}{mm^2}$; assuming as maximum acceptance voltage value $E = 15V$ and calculating current passing area, $450\ W$ power supply is needed.

For the preliminary phase a DC voltage power supply had been chosen (description in Appendix A.1).

2.3. Tool and tool holder

As already said the tool is a simple copper tube $\emptyset = 6\ mm$ diameter, it is connected by screw to a brass tube which internal diameter is $6\ mm$ and external is $16\ mm$; electric and electrolyte systems are linked by fast connectors to the brass tube, which acts as chamber to keep electrolyte pressure constant and ensure its supply continuity.

The tool as it is built is connected to the machine thanks to a collet chuck with Jacobs conical taper; an electrical insulating layer is interposed between them.

The machine is a CN mill equipped with step motors, which restrict the use for low speeds.

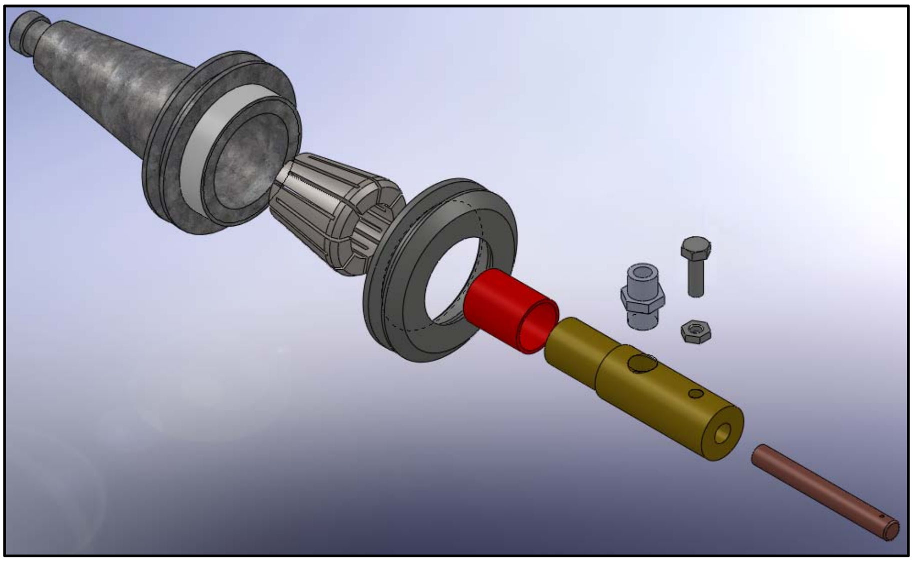

Image 2.6: Designed tool

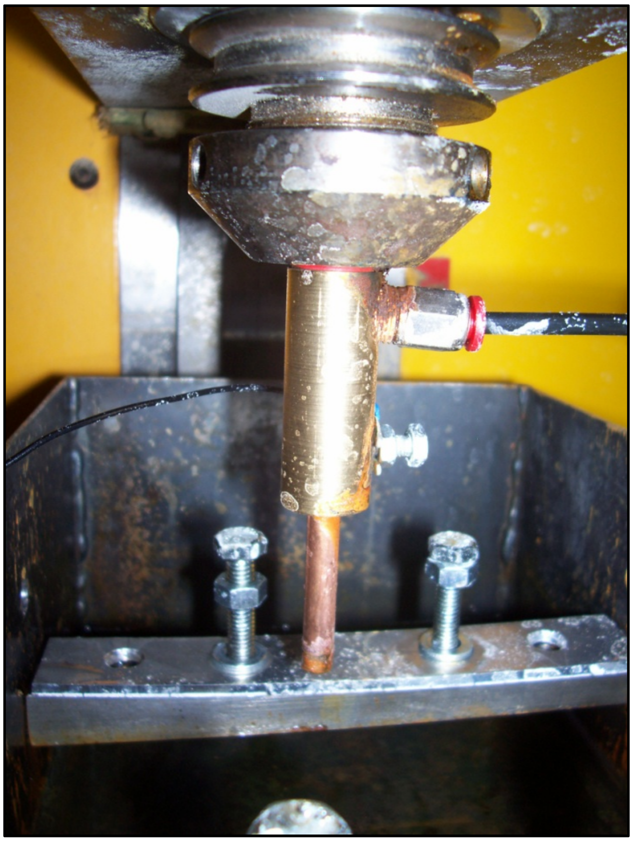

Image 2.7: Built tool

As a first step it has been decided not to insulate anyhow the tool and use the same formulas as expressed so far.

Pressures involved are low, so tool inflection calculation had been neglected.

2.4. Workpiece and workpiece holder

The workpiece holding system had been design to allow electrolyte collection after the working phase and avoid contacts between the workpiece and the fluid stored in the tank as showed in Image 2.8 and Image 2.9.

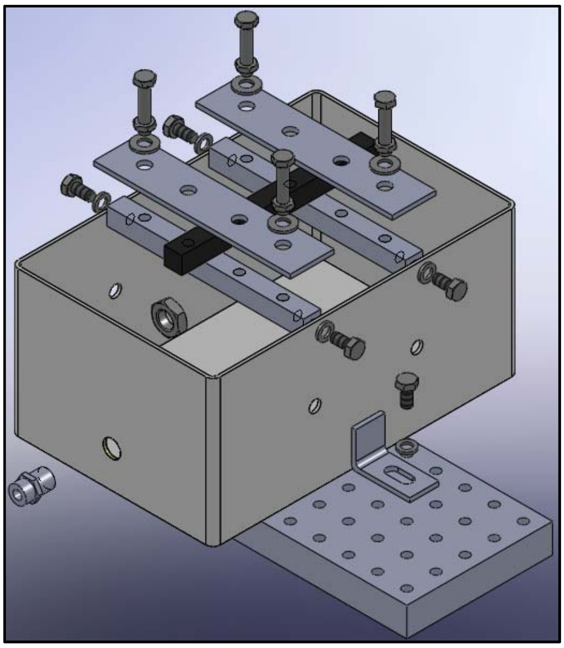

Image 2.8: Designed holding system

Image 2.9: Built holding system

Every machine sub-system has been designed and built; below is shown the assembled machine:

Image 2.10: Assembled system picture

3. Testing

Tests are made aiming on process parameter experimental extrapolation, achieving different steps:

- ***Steady tool and check if machining had taken place:***

  In this step gap and voltage had been modified to ensure machining workout

Chart 3.1

Test No.	Mark No.	Depth	Voltage	g_0	t
1	-	5	12	1.5	-
2	-	5	12	0.5	-
3	1	5	16	0.5	-
4	2	5	16	0.31	-
5	3	5	16	0.19	-

- ***Electrolyte concentration increasing and check:***

  The best result from the previous step had been taken and tool depth had been modified

6	4	5	16	0.31	-
7	5	5.5	16	0.31	-

- ***Steady tool, 1 min of machining and check:***

  Done for comparing results to theoretical values

8	6	5.5	16	0.06	1'
9	-	3.46	16	0.06	1'
10	7	6	12	0.1	1'

- ***Gap modifying and check:***

  Voltage and time changed during working

11	8	5.5	12	0.1	1'
12	9	6.5	From 12 to 16	0.31	1'45''

- ***Electrolyte speed modification:***

  Tried to use a flow grazing the side face as showed on Image 3.4Image 3.3

13	10	3.42	12	0.81	1'
14	-	4.49	12	0.68	1'

- ***Manual feeding, 5 seconds a step:***

  Time to work given

15	11	2.9	12	0.24	-
16	12	3.93	12	0.5	-

- ***Electrolyte concentration increasing up to 12% and 5 seconds steps manual feeding:***

  Tool depth modified

17	13	**3.99**	12	**0.5**	-

- ***Manual feeding taking care of amperometer constancy:***

  Gap and depth modified until they allowed a steady state process

18	14	**3.67**	13	**0.43**	-
19	15	**4.25**	13	**0.21**	1'30''
20	16	**4.1**	13	**0.21**	2'08''
21	17	**4.03**	13	**0.11**	2'08''
22	-	**4.32**	13.5	**0.11**	1'25''
23	-	**4.03**	13.5	**0.11**	2'55''
24	-	**4.03**	13.5	**0.1**	2'34''
25	-	**4.03**	13.5	**0.5**	6'40''
26	18	**4**	13.5	**0.36**	15'56''
27	19	**4**	13.5	**0.36**	7'05''
28	20	**4**	13	**0.36**	38'41''

After every test the workpiece had been removed and visually analyzed; then it had been placed again in the working area, needing tool offset setup.

The most relevant results had been marked and photographed (Image 4.1).

Tool offset setup had been made in the following way:

A piece of paper had been put between the tool and the workpiece; the tool had been moved through one axis till the paper wasn't nipped. The operation had been repeated for both of the axes left as well.

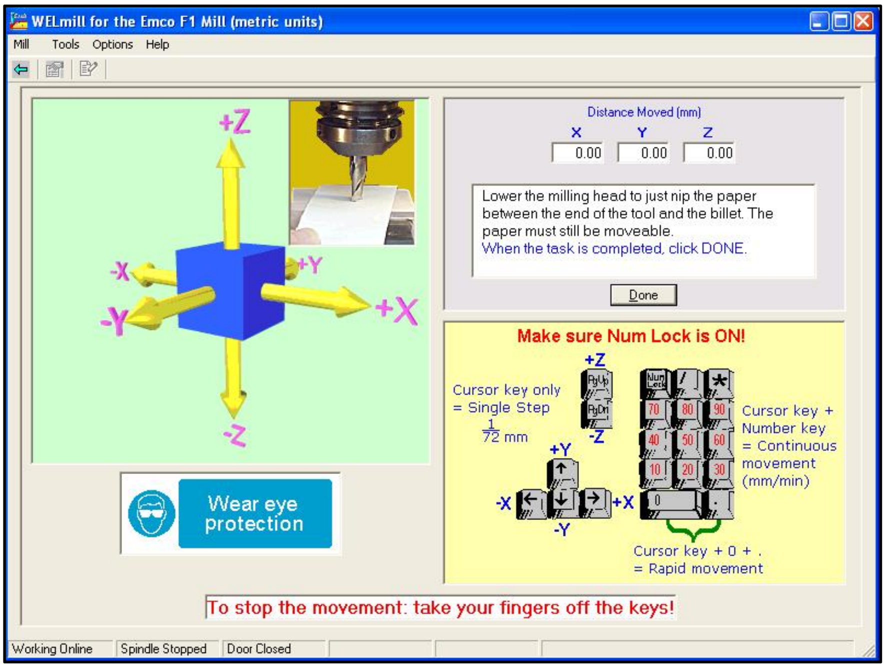

Image 3.1: Offset setup software frame

Pictures from testing:

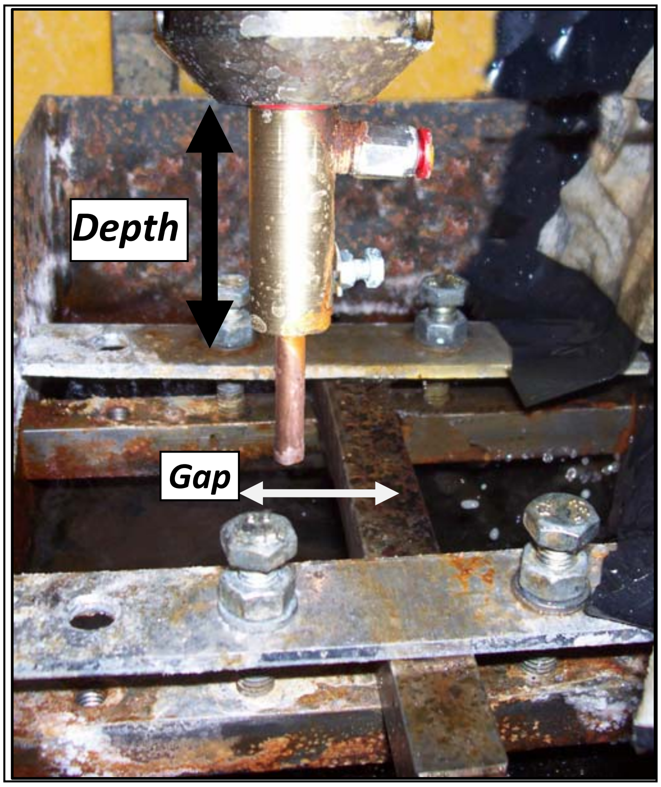

Image 3.2: Working parameters

Image 3.3: Amperometer check and voltage regulation

Image 3.4: Flow grazing side face

Image 3.5: Progressing machining

4. Evaluating

Following the pictures of the marked machinings are attached, every number is connected to the working parameters noted in Chart 3.1.

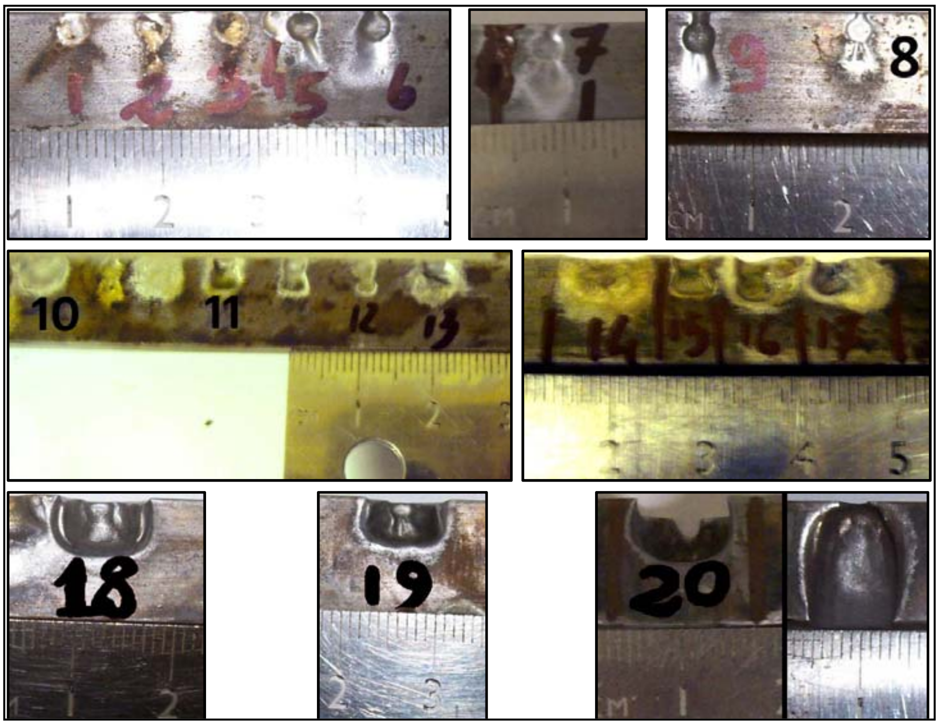

Image 4.1

First steps are characterized by high range of working parameters.

Tool depth has been modified as it could achieve the machining along all the sunk part, best results have been obtained when the hole where the electrolyte was going out from was at the same level of the top face, so outgoing fluid has split in two directions.

Since the thirteenth test the valve was partially open to slow down electrolyte speed; this choice has been made because the electrolyte bounced on workpiece face allowing the machining only in a restricted area; evolved sprinkles hit the tool and created an electric bridge between it and the machine, short-circuiting.

Last tests aimed to keep the current constant on a set value, which has been increased during the machining (as shown on Image 3.3 and Image 4.2)

From the comparison between real and ideal values comes out an high current density difference.

Since electrolyte didn't have proper characteristics due to filtering and flow speed problems, it can have assumed higher resistivity than the designed one (Chart 4.1).

In the Chart 4.1 gap value has been deduced mathematically as it is inverse proportional to the current increasing.

Current increasing comes from the better availability on working with gaps smaller and smaller.

A reason could be the electrolyte directionality which is proper after an unbalanced phase, so it allows to get the steady state. Available current is limited by the power supply, too few powerful to achieve the aim.

Last test brought to a nearly full machined slot creation, marked with no.20 and showed on Image 3.5; complete machining hasn't been possible due to the position of the hole where the electrolyte was outgoing from: it had reached and gone beyond the opposite face, therefore surrounding areas weren't fed with electrolyte, so current transfer stopped.

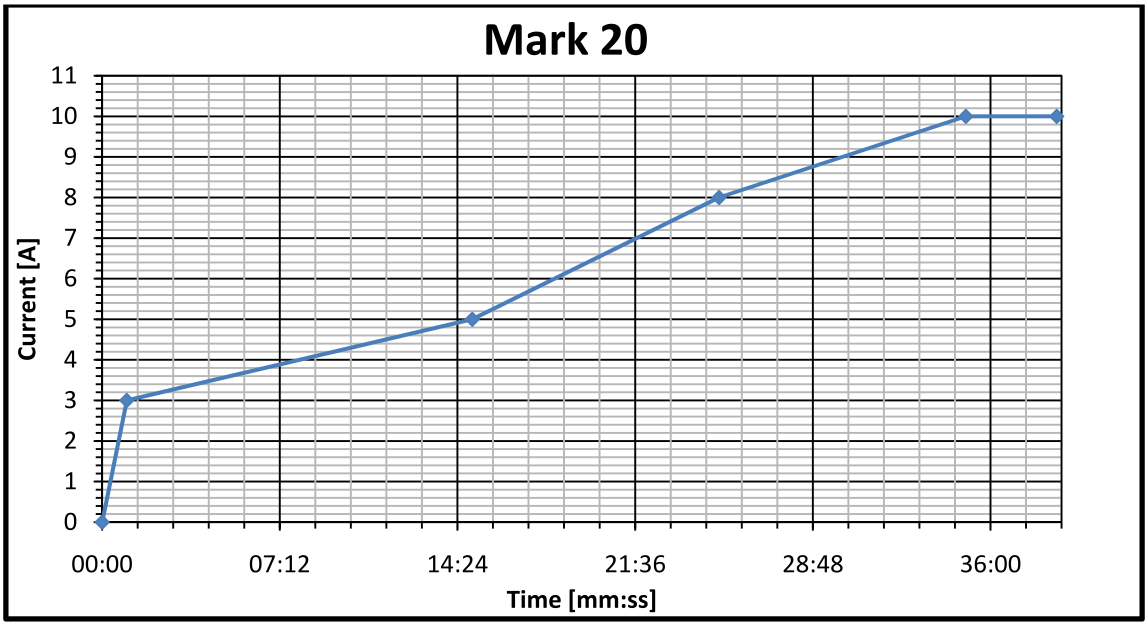

Image 4.2: Current increasing during test

Chart 4.1

E [V]	η	r [Ω·mm]	**g_0 [mm]**	t [mm:ss]	**I [A]**	Ideal Current density [A/mm^2]	**Real Current density [A/mm^2]**	Real Resistivity [Ω·mm]
13	**0.8**	0.5	**0.36**	00:00	**0**	58	**0**	Infinite
13	**0.8**	0.5	**0.36**	01:00	**3**	58	**0.08**	454
13	**0.8**	0.5	**0.36**	15:00	**5**	58	**0.1**	272
13	**0.8**	0.5	**0.36**	25:00	**8**	58	**0.2**	170
13	**0.8**	0.5	**0.36**	35:00	**10**	58	**0.3**	136

Overcut check hasn't been made due to big approximations done; saving it for checks after further developments.

Last tests show that the process can be repeated if basic working parameters are under control, achieving similar results.

The method can be standardized passing from manual control to electronic control in this doing:

- Using a pump allowing electronic flow speed regulation and electrolyte speed check as feed-back control;
- Checking gap and current constancy with feed-back loop control system;
- Using high precision slot measuring system, like laser or electronic microscope.

5. Conclusions and future work

Satisfying results had been obtained despite of system simplicity, proving process feasibility.

A way to intensify current transfer has to be studied, focusing on:

- Working area ingoing and out coming electrolyte temperature check;
- Fluid dynamic studying to improve electrolyte directionality;
- Modifying electrolyte outlet or its feeding from outside the tool;
- More powerful AC power supply;
- Electrolyte changing, rather using $NaNO_3$ solution;
- Using a more meshed filter;
- Tool inflection and its own frequencies measuring and determining their effects on the machining.

6. References

[1] M. Purcar, L. Bortels, B. Van den Bossche, J. Deconinck: *3D electrochemical machining computer simulations,* Journal of Materials Processing Technology 149 (2004) pp. 472–478.

[2] J. F. Thorpe, R. D. Zerkele: *Analytic determination of the equilibrium electrode gap in electrochemical machining*, Int. J. Mach. Tooi Des. Res. VoI. 9 (1969) pp. 131-144.

[3] M. Wang, W. Peng, C. Yao, Q. Zhang: *Electrochemical machining of the spiral internal turbulator*, Int J Adv Manuf Technol Vol. 49 (2010) pp. 969–973.

[4] N. Taniguchi: *Current Status in, and Future Trends of, Ultraprecision Machining and Ultrafine Materials Processing*, Annals of the ClRP Vol. 32/2/1983 pp. 573-582.

[5] S. H. Ahn, S. H. Ryu, D. K. Choi, C. N. Chu: *Electro-chemical micro drilling using ultra short pulses*, Precision Engineering 28 (2004) pp. 129–134.

[6] Prof. Dr.- Ing. F. Klocke: *Lecture in the Subject: Manufacturing Technology I Material Removing Techniques*, pag. 41.

[7] L. Bortels, M. Purcar, B. Van den Bossche, J. Deconinck: *A user-friendly simulation software tool for 3D ECM*, Journal of Materials Processing Technology 149 (2004) pp. 486–492.

[8] J. Kozak, L. Dabrowski, K. Lubkowski, M. Rozenek, R. SøawinÂski: *CAE-ECM system for electrochemical technology of parts and tools*, Journal of Materials Processing Technology 107 (2000) pp. 293-299.

[9] Y. G. Tsuei , R. H. Nilson: *Effects of variable electrolyte conductivity on side gap geometry in ECM*, Int. J. Mach. Tool Des. Res. Vol. 17 (1977) pp. 169-178.

[10] V. K. Jain and K. P. Rajurkar: *An integrated approach for tool design in ECM*, Precision engineering (1991) pp. 111-124.

[11] W. Natsu, T. Ikeda, M. Kunieda: *Generating complicated surface with electrolyte jet machining*, Precision Engineering Vol. 31 (2007) pp. 33–39.

[12] B. H. Kim, S. H. Ryu, D. K. Choi, C. N. Chu: *Micro electrochemical milling*, Journal of micromechanics and microengineering Vol. 15 (2005) pp. 124–129.

[13] V. K. Jain, P. C. Pandey: *Tooling design for ecm*, Precision Engineering (1980) pp. 195-206.

[14] D. Clifton, A.R. Mount, G.M. Alder, D. Jardine: *Ultrasonic measurement of the inter-electrode gap in electrochemical machining*, International Journal of Machine Tools & Manufacture Vol. 42 (2002) 1259–1267.

[15] A. K. M. De Silva, H. S. J. Altena, J. A. McGeough: *Influence of electrolyte concentration on copying accuracy of precision ECM*, Annals of the CIRP Vol. 52/1/2003 pp. 165-168.

[16] R. Förster, A. Schoth, W. Menz: *Micro-ECM for production of Microsystems with a high aspect ratio*, Microsystem Technologies Vol. 11 (2005) pp. 246-249.

[17] J. Pattavanitch, S. Hinduja, J. Atkinson: *Modeling of the electrochemical machining process by the boundary element method*, Annals of the CIRP Vol. 59 (2010) pp. 243-246.

[18] V. K. Jain, P. C. Pandey: *Tooling design for ECM*, Precision engineering (1980) pp. 195-206.

[19] A. De Silva, T. Pajak, K. Mediliyegedara: *Investigation of the process principles and mechanism of Electrochemical Milling (ECMIL)*, Glasgow Caledonian University internal report (2010) pp. 1-11.

[20] J. F. Wilson: *Practice and theory of electrochemical machining*, ed. Wiley-Interscience 1971, pag. 252

[21] H. S. J. Altena: *Precision ECM by process characteristic modeling*, Glasgow Caledonian University thesis for the degree of Doctor of Philosophy (2000) pag. 251

Appendix

A.1. Power supply order

Palstar PS30M

30 Amp Variable Power Supply

Description

Palstar PS-30M - 25 - 30 Amp Variable Voltage Power Supply. One of our most popular power supplies.

Designed for a variety of applications, this power supply is ideal for powering most HF transceivers where protection, reliability and immunity to RF are important. This is a high quality variable voltage power supply utilising galvanised steel case, precision ammeter and voltmeter monitoring. Thermostatically controlled fan, H/D screw terminals and convenient snap in terminals. The supply has short circuit protection
and has an overcurrent warning indicator.

- **Palstar PS-30M:** Variable Voltage Power Supply
- **Input voltage**: 220/240V AC
- **Output voltage:** 3-15V DC adjustable
- **Current**: 25/30A Max.
- **Noise and ripple:** 10mV RMS
- **Thermostatically** controlled fan
- **Volt** and current metering
- **Overcurrent** warning indication
- **Short circuit** protection
- **Weight:** 8.58kg
- **Size:** 150 x 145 x 300mm
- **Manson model** - EP-925

A.2. Bill of materials

Electrical system

0-15 V; 0-30 A variable power supply .... ☐

Wires .... ☐

Connectors to the tool and the workpiece .... ☐

Volt meter .... ☐

Electrolyte system

15 bar pump .... ☐

2 tanks .... ☐

Filter .... ☐

Tubes (10 mm diameter) .... ☐

4 Valves .... ☐

Water .... ☐

$NaNO_3$ .... ☐

Tool and tool holder

Brass bar .... ☐

Copper tube .... ☐

Collet chuck (with taper) .... ☐

A.3. Drawings

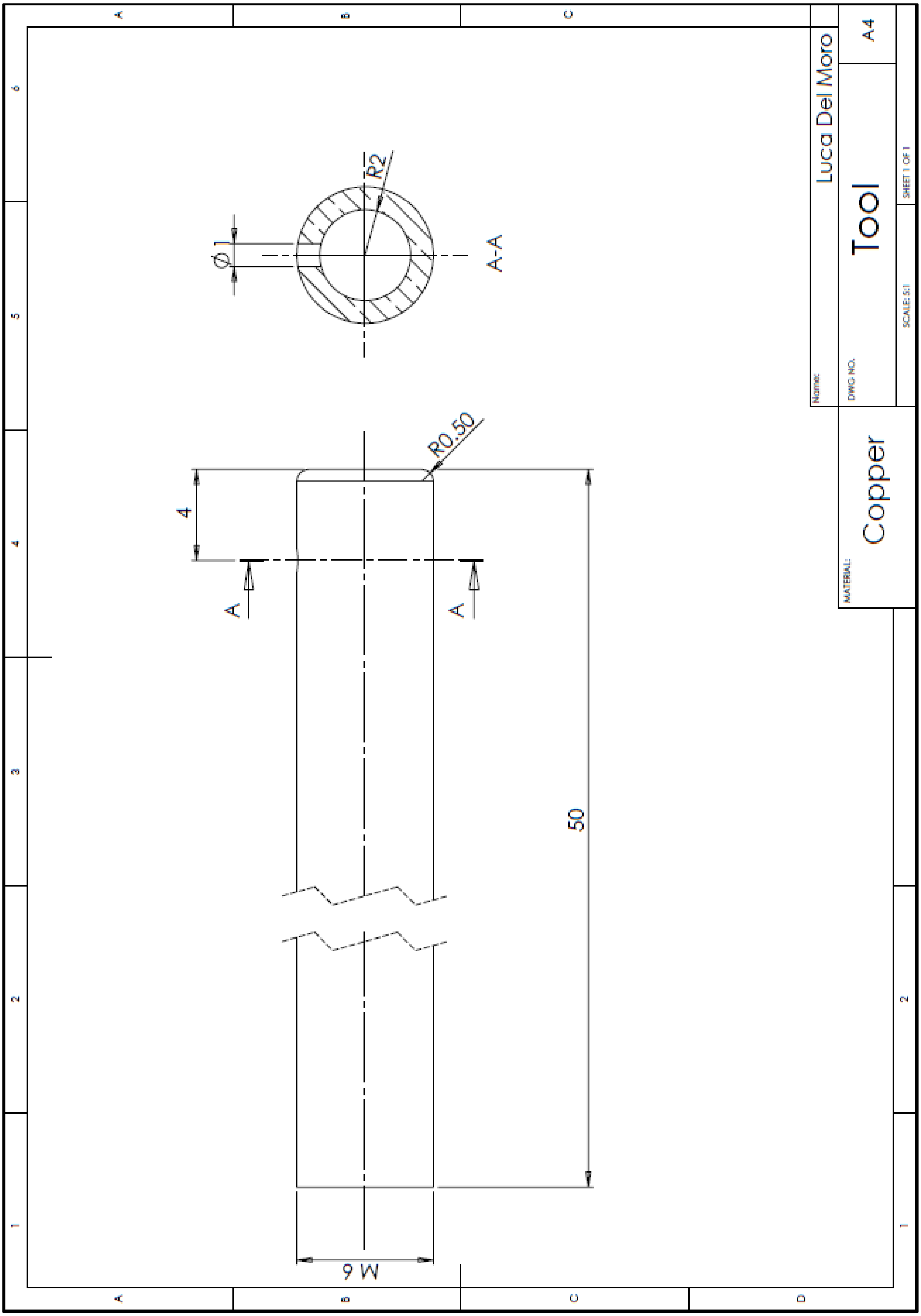
Luca Del Moro
A4
Tool
SHEET 1 OF 1
SCALE: 5:1
Name:
DWG NO.
MATERIAL:
Copper
R2
Ø 1
A-A
R0.50
4
A
A
50
M 6

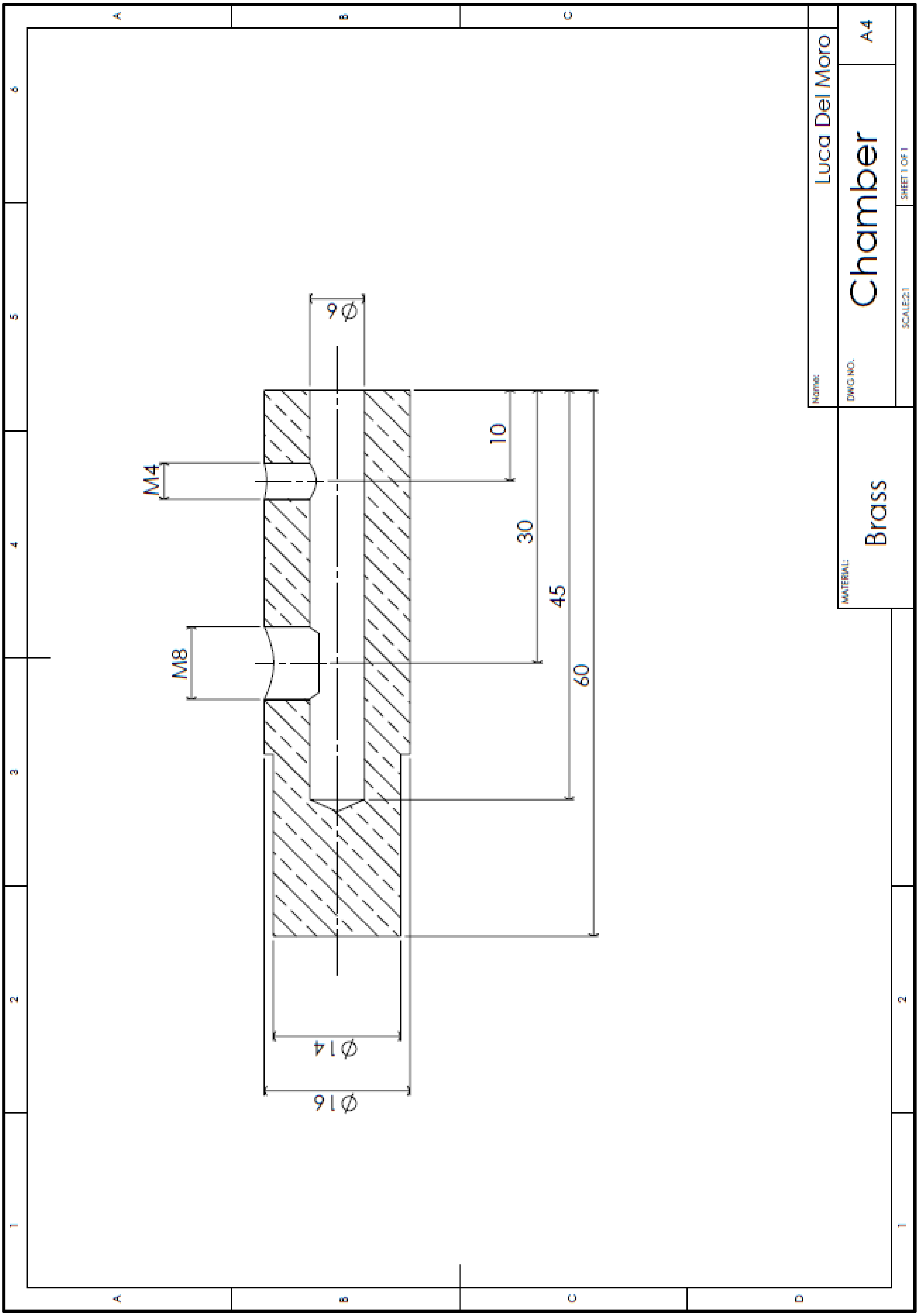
Name:
Luca Del Moro
DWG NO.
Chamber
A4
SCALE:2:1
SHEET 1 OF 1
MATERIAL:
Brass
Ø6
M4
M8
10
30
45
60
Ø14
Ø16

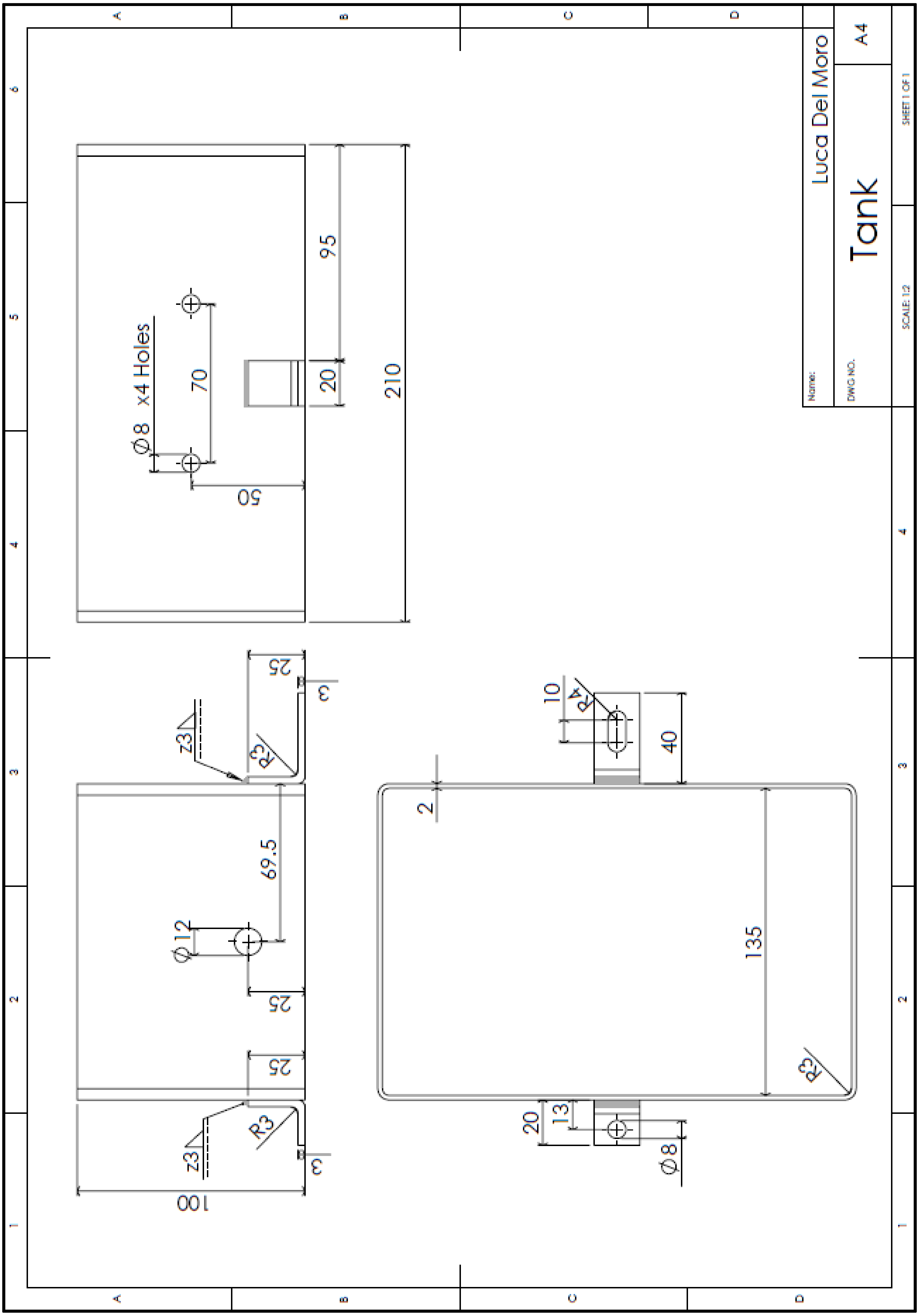
Luca Del Moro
Tank
A4
Name:
DWG NO.
SCALE: 1:2
SHEET 1 OF 1
Ø8 x4 Holes
70
95
20
210
50
25
3
Z3
R3
69.5
Ø12
100
2
135
10
R4
40
20
13
Ø8

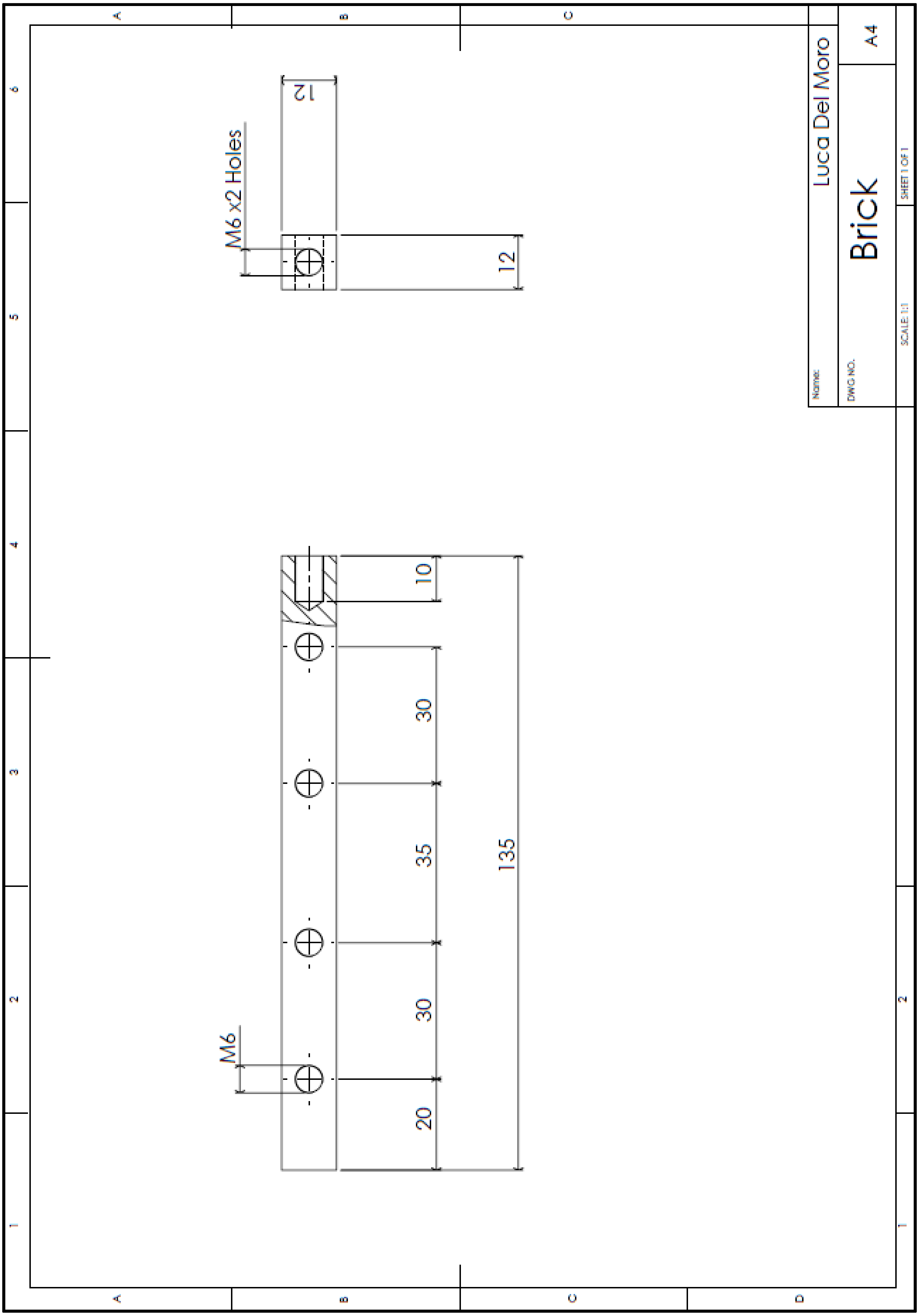
Luca Del Moro
Brick
A4
Name:
DWG NO.
SCALE: 1:1
SHEET 1 OF 1
M6 x2 Holes
12
12
M6
10
30
35
30
20
135

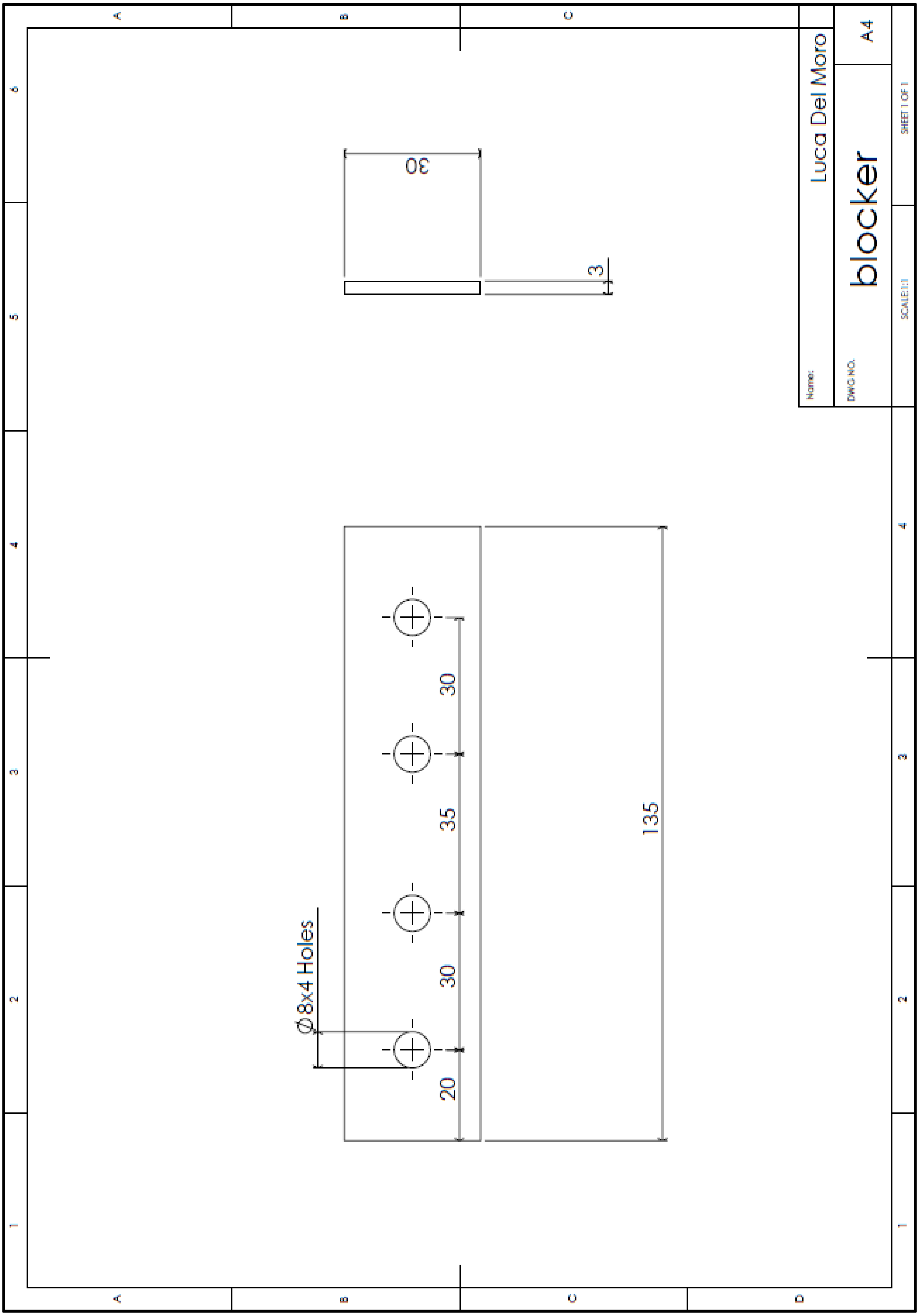

Luca Del Moro
A4
Name:
DWG NO.
blocker
SCALE1:1
SHEET 1 OF 1
30
3
Ø8x4 Holes
20
30
35
30
135